

# Spectroscopic study of $\text{N}_2\text{O}^+(\text{A } ^2\Sigma^+)$ by photofragment excitation spectrum

Haifeng Xu, Ying Guo, Qifeng Li, Shilin Liu,<sup>a)</sup> and Xingxiao Ma  
*Open Laboratory of Bond Selective Chemistry, Department of Chemical Physics,  
University of Science and Technology of China, Hefei, Anhui 230026, China*

Jun Liang and Haiyang Li  
*Anhui Institute of Optics and Fine Mechanics, Chinese Academy of Science, Hefei, Anhui 230031, China*

(Received 20 June 2003; accepted 16 September 2003)

Photofragment  $\text{NO}^+$  excitation spectrum of  $\text{N}_2\text{O}^+$  ions has been studied in the wavelength range of 278–328 nm, where the parent  $\text{N}_2\text{O}^+$  ions were state-selectively prepared at the  $X^2\Pi_{1/2,3/2}(000)$  levels by  $[3+1]$  multi-photon ionization of jet-cooled  $\text{N}_2\text{O}$  molecules at 360.55 nm. The spectrum was attributed completely to the  $\text{A } ^2\Sigma^+ \leftarrow X^2\Pi_{3/2,1/2}(000)$  electronic transition of  $\text{N}_2\text{O}^+$ . Totally 47 vibronic bands associated to 24 vibrational levels of the  $\text{A } ^2\Sigma^+$  state were identified in the present work, most of which were observed for the first time. The sufficient spectroscopic data made it possible to investigate the Fermi-resonance between the  $\nu_1$  and  $\nu_2$  vibrational modes at the  $\text{A } ^2\Sigma^+$  state. Based on the assignment, the spectral constants of the  $\text{A } ^2\Sigma^+$  state, such as vibrational frequencies, anharmonic constants, and Fermi interaction constant, were determined with relatively high reliability and precision. © 2003 American Institute of Physics. [DOI: 10.1063/1.1624596]

## I. INTRODUCTION

The  $\text{N}_2\text{O}^+$  molecular ion plays an important role in the ionosphere as it is the intermediate in the reaction of  $\text{O}^+$  and  $\text{N}_2$ ,<sup>1,2</sup> and thus has been investigated by a lot of experimental techniques, such as fluorescence emission spectrum,<sup>3–10</sup> fast ion beam laser spectroscopy (FIBLAS),<sup>11–16</sup> laser induced fragment,<sup>17</sup> and photoelectron spectroscopy.<sup>18–20</sup> Extensive studies have been performed to the electronic ground-state  $X^2\Pi$ , and have revealed many complex spectroscopic features arising from various interactions, such as the spin-orbit splitting, Renner-Teller interactions, and the Fermi-resonance couplings in the  $X^2\Pi$  state.<sup>3–5,16,21,22</sup>

The first electronically excited state of  $\text{N}_2\text{O}^+$ ,  $\text{A } ^2\Sigma^+$ , however, has not been studied sufficiently and systematically compared to the electronic ground state. Up to now, the vibrational structure of  $\text{A } ^2\Sigma^+$  state has not yet been investigated in detail. Previous emission studies have showed that except for ground vibrational level, all the excited vibrational levels of  $\text{A } ^2\Sigma^+$  state undergo a predissociation process, therefore, only a limited number of the lowest vibrational levels have been investigated via fluorescence emission spectroscopy.<sup>3–10</sup> Larzilliere *et al.*<sup>11–16</sup> have investigated several lowest levels of the  $\text{A } ^2\Sigma^+$  state in detail with highly resolved rovibrational FIBLAS spectroscopy. Very recently, Ng and co-workers<sup>18</sup> performed a vacuum ultraviolet pulsed field ionization-photoelectron (PFI-PE) study, and have observed some new vibrational levels of the  $\text{A } ^2\Sigma^+$  state.

Despite of extensive works regarding the  $X^2\Pi$  state and several lowest vibrational levels of the  $\text{A } ^2\Sigma^+$  state, there has been very few reports about the high vibrational levels of the

$\text{A } ^2\Sigma^+$  state, especially levels higher than the (300) level. Since the vibrational frequencies of the  $\text{A } ^2\Sigma^+$  state have the relations  $\nu_3 \sim 2\nu_1 \sim 4\nu_2$  as determined by several independent works,<sup>3,18,19</sup> Fermi-resonance couplings are expected to occur among vibrational levels  $(V_1, V_2, V_3)$ ,  $(V_1-1, V_2+2, V_3)$  and  $(V_1-2, V_2, V_3+1)$ . However, the Fermi-resonance interaction as well as the anharmonic effect of the  $\text{A } ^2\Sigma^+$  state have not yet been investigated, presumably due to the insufficiency of available spectroscopic data. In this study, we prepared  $\text{N}_2\text{O}^+$  at the vibrational ground level of the  $X^2\Pi$  state through  $[3+1]$  resonance-enhanced multi-photon resonant ionization (REMPI) of neutral  $\text{N}_2\text{O}$  molecules, and excited the generated  $\text{N}_2\text{O}^+$  ions to the  $\text{A } ^2\Sigma^+$  state with another laser. By monitoring the  $\text{NO}^+$  fragments from the dissociation of  $\text{N}_2\text{O}^+(\text{A } ^2\Sigma^+)$  and scanning the excitation laser in the wavelength range of 278–328 nm, a photofragment excitation spectrum (PHOFEX) was obtained. The PHOFEX spectrum reveals many new vibronic bands, which were not observed in previous studies, therefore, makes the assignments more reliable, and enables us to determine the Fermi-resonance couplings as well as the spectral constants about the  $\text{A } ^2\Sigma^+$  state with relatively high precision.

## II. EXPERIMENT

The experimental setup has been described in detail previously.<sup>23</sup> Briefly, the  $\text{N}_2\text{O}^+$  ions were prepared by the frequency doubled output of a dye laser through  $[3+1]$  REMPI of jet-cooled  $\text{N}_2\text{O}$  molecules, and then were excited to the  $\text{A } ^2\Sigma^+$  electronic state by another dye laser. The photofragment ions,  $\text{NO}^+$ , were detected by a home-made time-of-flight (TOF) mass spectrometer.

<sup>a)</sup> Author to whom correspondence should be addressed. Electronic mail: slliu@ustc.edu.cn

The jet-cooled  $\text{N}_2\text{O}$  molecules were produced from supersonic expansion of  $\text{N}_2\text{O}/\text{He}$  (20%) gas mixture through a pulsed nozzle with duration of 200  $\mu\text{s}$  and orifice diameter of 0.5 mm into a main vacuum chamber. The chamber was pumped by two turbo-molecule pumps (1500 l/s), which were backed up by two mechanical pumps (70 and 15 l/s, respectively). The stagnation pressure was kept at  $\sim 2$  atm, and the operating pressures in the chamber was about  $1 \times 10^{-6}$  Torr.

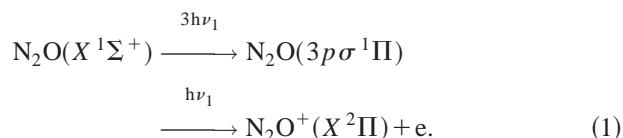
Two dye lasers (PRSC-LG-18 and PRSC-LG-24, Sirah), pumped simultaneously by the second harmonic output of a Nd:YAG laser (PRO-190, Spectra Physics), were employed in this experiment. The frequency doubled output of one dye laser,  $\sim 3$  mJ/pulse, was used as the ionization light source to generate  $\text{N}_2\text{O}^+(X^2\Pi)$  ions by focusing perpendicularly on the  $\text{N}_2\text{O}$  molecular beam with a quartz lens of  $f=300$  mm. The wavelength of the ionization laser was fixed at 360.55 nm which corresponds to the three photon resonant Rydberg transition of  $\text{N}_2\text{O}$ ,  $3p\sigma^1\Pi \leftarrow \leftarrow \leftarrow X^1\Sigma$ .<sup>24,25</sup> The frequency doubled output of another dye laser,  $\sim 1$  mJ/pulse, counter-propagating with the ionization laser and focused with a quartz lens of  $f=600$  mm, was operated in the wavelength range of 278–328 nm to excite  $\text{N}_2\text{O}^+$  ions from the  $X^2\Pi$  state to the  $A^2\Sigma^+$  state.

The produced ions, including parent  $\text{N}_2\text{O}^+$  ions and fragment  $\text{NO}^+$  ions, were detected with a home-made TOF mass spectrometer. The ion signals were amplified with a pre-amplifier, and the mass-resolved data were collected by averaging the amplified signals for selected mass species with boxcar averagers (Stanford SR250), and interfaced to a PC for data storage. During the experiment, the intensities of both lasers were monitored simultaneously with two photodiodes, and the wavelength of the excitation laser was calibrated simultaneously against the argon optogalvanic spectrum resulting in an overall absolute uncertainty of  $\sim 0.5$   $\text{cm}^{-1}$  in the excitation energy. Both lasers were temporally and spatially overlapped with each other in the molecule–laser interaction region.

### III. RESULTS AND DISCUSSIONS

#### A. Overall TOF mass spectrum

Figure 1(a) shows the TOF mass spectrum obtained with the ionization laser only, by fixing the wavelength at  $\lambda=360.55$  nm and maintaining the pulse energy at  $\sim 3$  mJ. The  $[3+1]$  REMPI of  $\text{N}_2\text{O}$  in this wavelength region had been studied in detail by Szarka *et al.*<sup>24</sup> and Scheper *et al.*<sup>25</sup> The wavelength of 360.55 nm used in this study corresponds to a single transition band in the  $[3+1]$  REMPI spectrum, which can be expressed as,



It can be seen clearly in the mass spectrum that  $\text{N}_2\text{O}^+$  ions are the predominant products formed by  $[3+1]$  REMPI at this wavelength, and the amount of  $\text{NO}^+$  fragment ions are less than 0.1% of the  $\text{N}_2\text{O}^+$  ions. As stated by Szarka *et al.*,<sup>24</sup>  $\text{NO}^+$  ions in the REMPI experiment come from the

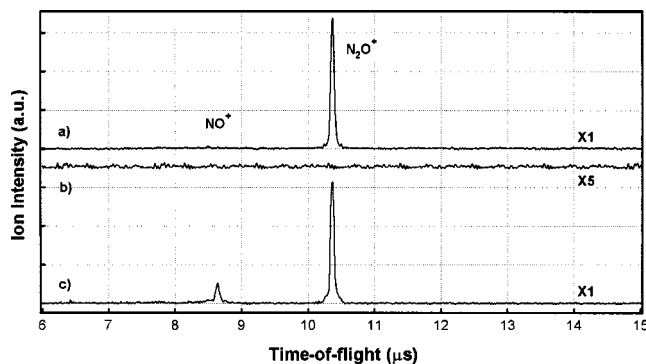


FIG. 1. The TOF mass spectrum with (a) only the photoionization laser at 360.55 nm; (b) only the excitation laser at 305.82 nm and (c) both the ionization and excitation lasers overlapped temporally and spatially with each other. The  $\text{N}_2\text{O}^+$  ions in (a) and (c) were generated via  $[3+1]$  REMPI of  $\text{N}_2\text{O}$  molecules by the ionization laser, and the  $\text{NO}^+$  ions in (c) were produced from dissociation of  $\text{N}_2\text{O}^+$  ions by the excitation laser. The pulse energies of the ionization laser and dissociation laser were optimized and maintained at  $\sim 3$  and  $\sim 1$  mJ, respectively.

subsequent nonresonant two-photon ionization of neutral NO from the dissociation of  $\text{N}_2\text{O}$  ( $3p\sigma^1\Pi$ ). This means we could achieve soft ionization to prepare pure  $\text{N}_2\text{O}^+$  ions. Scheper *et al.*<sup>25</sup> showed in their REMPI-photoelectron study that the  $\text{N}_2\text{O}^+$  ions produced via  $[3+1]$  REMPI at 360.55 nm are populated totally at the vibrationless electronic ground state, i.e.,  $X^2\Pi_{1/2}(000)$  and  $X^2\Pi_{3/2}(000)$ . Despite the mechanism in detail, we could certainly prepare exclusive and state-selective  $\text{N}_2\text{O}^+$  ions in the  $X^2\Pi(000)$  state with minimum fragment  $\text{NO}^+$  by using a lens with middle focus length and optimizing the pulse energy of ionization laser at  $\sim 3$  mJ.

By introducing another laser to excite the prepared  $\text{N}_2\text{O}^+$  ions, a PHOFEX spectrum of  $\text{N}_2\text{O}^+$  could be obtained. As shown in Fig. 1(b), only with the excitation laser no ion signal could be observed by carefully controlling the laser intensity. However, with combination of the ionization and excitation lasers, a remarkable  $\text{NO}^+$  signal was observed in Fig. 1(c). In the entire excitation wavelength region,  $\text{NO}^+$  ions are the dominant fragments. As indicated by Szarka *et al.*,<sup>24</sup> it is possible that the  $\text{NO}^+$  could come from ionization of the  $\text{N}_2\text{O}(3p\sigma^1\Pi)$  dissociation product, by subsequently absorbing two photons of the excitation laser. We excluded this possibility and confirmed that the  $\text{NO}^+$  ions are generated completely from the excitation of parent  $\text{N}_2\text{O}^+$  ions, by varying the temporal delay and the spatial overlap of the two lasers. In the wavelength range of the excitation laser employed in present work,  $\text{N}_2\text{O}^+$  ions at the  $X^2\Pi(000)$  state could be excited to the  $A^2\Sigma^+$  state through one-photon absorption. The power dependence of  $\text{NO}^+$  signal on the intensity of excitation laser was measured, and the power dependence index was found around 0.5. A  $[1+1]$  excitation–dissociation scheme via the  $A^2\Sigma^+$  state could not happen, since under present experimental conditions the excitation photon flux is less than  $10^{24}$  photon/ $\text{cm}^2/\text{s}$ , even if the further excitation cross section from the  $A^2\Sigma^+$  state is as large as  $10^{-18}$   $\text{cm}^2$ , the rate of second excitation step is still less than  $10^6$   $\text{s}^{-1}$ , which can not compete with the dissociation rate of the  $A^2\Sigma^+$  state (higher than  $10^8$   $\text{s}^{-1}$ ).<sup>9</sup> Therefore, the

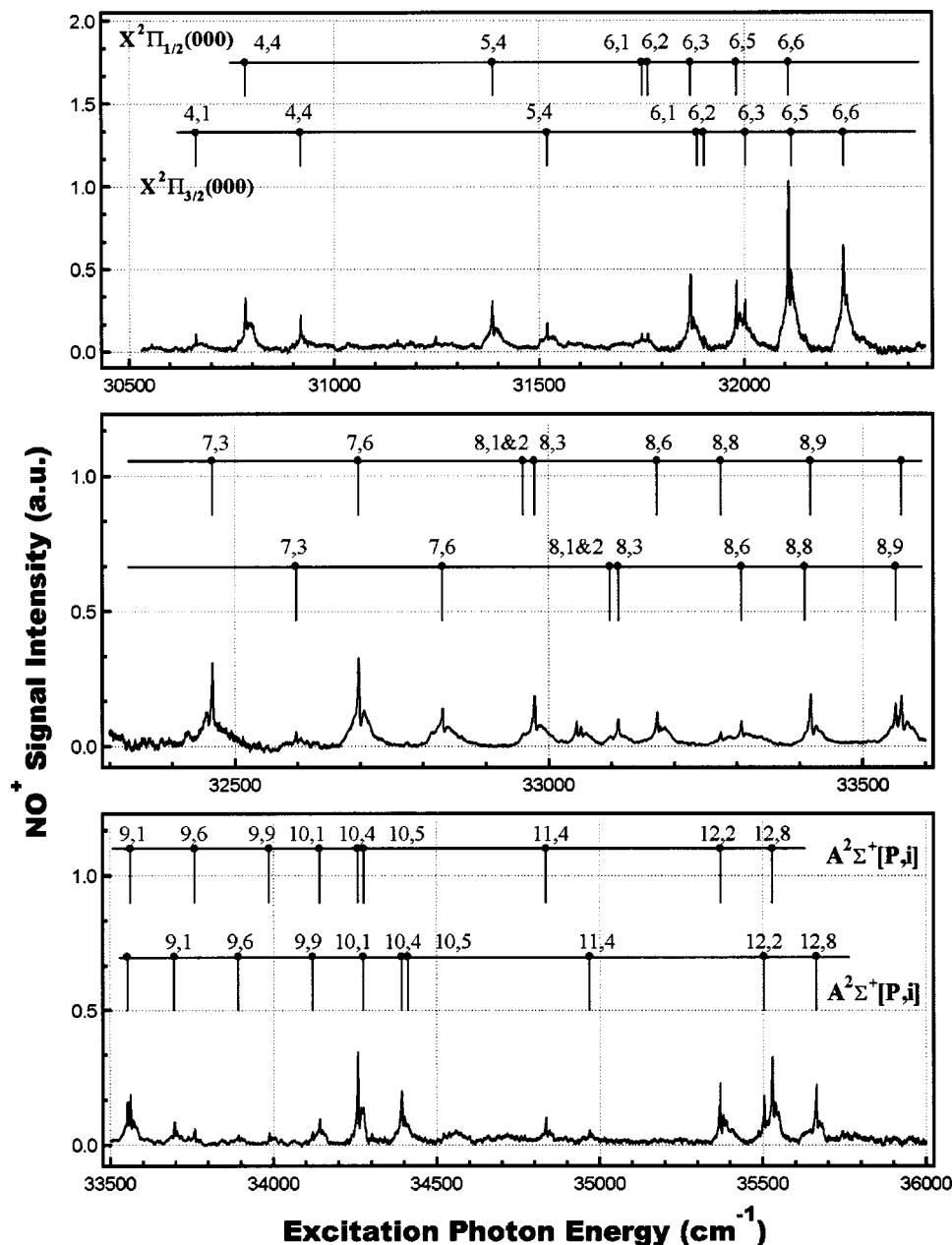


FIG. 2. The PHOFEX spectrum of  $\text{N}_2\text{O}^+$  obtained by monitoring  $\text{NO}^+$  fragment in the wavelength range of 275–328 nm, which is attributed to  $A^2\Sigma^+ \leftarrow X^2\Pi_{1/2,3/2}(000)$  electronic transition and assigned in terms of Fermi-resonance coupled vibrational levels in the  $A^2\Sigma^+$  state. The spectrum consists of many newly observed vibronic bands, making the assignment more reliable and the determined spectral constants more precise.

$\text{NO}^+$  signal in Fig. 1(c) should be the dissociation product of  $\text{N}_2\text{O}^+$  at the  $A^2\Sigma^+$  state. A scan of the excitation laser while monitoring the  $\text{NO}^+$  signal intensity could enable us to obtain a photofragment excitation (PHOFEX) spectrum, and then the spectroscopic information about the  $A^2\Sigma^+$  state could be derived from the spectrum.

### B. Analysis of the PHOFEX spectrum

Figure 2 shows the  $\text{NO}^+$  PHOFEX spectrum in the wavelength range of 278–328 nm which has been corrected for the variation of excitation laser intensity. Due to the different experimental technique employed in this work, the present spectrum reveals many new vibronic features, which were not observed in all previous studies regarding the  $A^2\Sigma^+$  state of  $\text{N}_2\text{O}^+$ , and thus should make our spectral analysis more reliable and provide more detailed spectroscopic information about the  $A^2\Sigma^+$  state.

The  $A^2\Sigma^+$  state of  $\text{N}_2\text{O}^+$  ions is known to be linear, and has similar geometries to its electronic ground state  $X^2\Pi$ .<sup>21</sup> The vibrational frequencies  $\nu_1$  (symmetry stretching),  $\nu_2$  (bending), and  $\nu_3$  (anti-symmetric stretching) of  $\text{N}_2\text{O}^+(A^2\Sigma^+)$  are known to be around 1346, 611, and 2450  $\text{cm}^{-1}$ , respectively, as determined from the fluorescence emission study,<sup>3</sup> FIBLAS studies,<sup>11–16</sup> and photoelectron measurements.<sup>18</sup> Based upon the known vibrational frequencies of  $\text{N}_2\text{O}^+(A^2\Sigma^+)$  and several observed  $A^2\Sigma^+ \rightarrow X^2\Pi(000)$  vibronic transitions in emission studies, tentative assignments were performed to the PHOFEX spectrum. It was found that except for a few peaks in the low excitation energy region in Fig. 2, most of the transitions could not be assigned properly into excitations of  $\nu_1$ ,  $\nu_2$ , and  $\nu_3$  mode vibrational progressions of the  $A^2\Sigma^+$  state or their combinations, even if taking into account of the anharmonic constants.

TABLE I. Observed transitions in the PHOFEX spectrum and the corresponding assignments.

Band positions (cm <sup>-1</sup> )		Assignments <sup>a</sup>
This work	Ref. 17	
30 662.5	30 665.0	[4,1] ← (000)F <sub>1</sub>
30 783.5	30 776.8	[4,4] ← (000)F <sub>2</sub>
30 917.6	30 909.0	[4,4] ← (000)F <sub>1</sub>
31 386.1		[5,4] ← (000)F <sub>2</sub>
31 519.2		[5,4] ← (000)F <sub>1</sub>
31 750.2		[6,1] ← (000)F <sub>2</sub>
31 884.0		[6,1] ← (000)F <sub>1</sub>
31 766.8		[6,2] ← (000)F <sub>2</sub>
31 900.6		[6,2] ← (000)F <sub>1</sub>
31 869.2		[6,3] ← (000)F <sub>2</sub>
32 002.9		[6,3] ← (000)F <sub>1</sub>
31 980.7		[6,5] ← (000)F <sub>2</sub>
32 114.5		[6,5] ← (000)F <sub>1</sub>
32 107.8		[6,6] ← (000)F <sub>2</sub>
32 240.9		[6,6] ← (000)F <sub>1</sub>
32 463.8		[7,3] ← (000)F <sub>2</sub>
32 597.0		[7,3] ← (000)F <sub>1</sub>
32 697.0		[7,6] ← (000)F <sub>2</sub>
32 830.6		[7,6] ← (000)F <sub>1</sub>
32 965.0		[8,1&2] ← (000)F <sub>2</sub>
33 099.0		[8,1&2] ← (000)F <sub>1</sub>
32 977.2		[8,3] ← (000)F <sub>2</sub>
33 110.7		[8,3] ← (000)F <sub>1</sub>
33 172.7		[8,6] ← (000)F <sub>2</sub>
33 307.0		[8,6] ← (000)F <sub>1</sub>
33 274.4		[8,8] ← (000)F <sub>2</sub>
33 408.0		[8,8] ← (000)F <sub>1</sub>
33 417.1		[8,9] ← (000)F <sub>2</sub>
33 552.4		[8,9] ← (000)F <sub>1</sub>
33 562.0		[9,1] ← (000)F <sub>2</sub>
33 696.6		[9,1] ← (000)F <sub>1</sub>
33 758.4		[9,6] ← (000)F <sub>2</sub>
33 892.7		[9,6] ← (000)F <sub>1</sub>
33 988.0		[9,9] ← (000)F <sub>2</sub>
34 120.1		[9,9] ← (000)F <sub>1</sub>
34 141.9		[10,1] ← (000)F <sub>2</sub>
34 276.4		[10,1] ← (000)F <sub>1</sub>
34 258.6		[10,4] ← (000)F <sub>2</sub>
34 393.2		[10,4] ← (000)F <sub>1</sub>
34 278.0		[10,5] ← (000)F <sub>2</sub>
34 413.0		[10,5] ← (000)F <sub>1</sub>
34 835.5		[11,4] ← (000)F <sub>2</sub>
34 969.6		[11,4] ← (000)F <sub>1</sub>
35 369.5		[12,2] ← (000)F <sub>2</sub>
35 503.9		[12,2] ← (000)F <sub>1</sub>
35 529.3		[12,8] ← (000)F <sub>2</sub>
35 663.9		[12,8] ← (000)F <sub>1</sub>

<sup>a</sup>F<sub>1</sub> and F<sub>2</sub> correspond to the transitions from the ground states  $X^2\Pi_{3/2}(000)$  and  $X^2\Pi_{1/2}(000)$ , respectively.

In fact, since the vibrational frequencies of  $N_2O^+(A^2\Sigma^+)$  have the approximate relations  $\nu_3 \sim 2\nu_1 \sim 4\nu_2$ , Fermi-resonance interaction is expected to occur between the  $(V_1, V_2^l, V_3)$  and  $(V_1 - 1, (V_2 + 2)^l, V_3)$ , or  $(V_1, V_2^l, V_3)$  and  $(V_1 + 2, V_2^l, V_3 - 1)$  vibrational levels, where  $V_1$ ,  $V_2$ ,  $V_3$ , and  $l$  represent the vibrational quantum numbers of  $\nu_1$ ,  $\nu_2$ , and  $\nu_3$  modes and the vibrational angular momentum, respectively. Therefore, the Fermi interaction makes zero-order vibrational eigenstates mixed with each other, and it is unfeasible to perform the spectral assignment in normal way, especially for transitions to high vibrational

levels. As stated by Bernath *et al.*,<sup>26</sup> such a coupled cluster of zero-order vibrational levels can be represented by a polyad quantum number  $P$ , which is defined as  $P = 2V_1 + V_2 + 4V_3$  in present case. Then, only vibrational levels with the same  $P$  and  $l$  interact with each other. Since the zero-order levels in a polyad mix with each other by Fermi interaction, using expression  $(V_1, V_2, V_3)$  to label the vibrational level will lose its meaning, we therefore refer to the eigenstates as  $[P, i]$ , where  $i$  represents the energy ordering number within the polyad increasing with the energy.

Due to the Fermi interaction in the  $A^2\Sigma^+$  state, the vibrational energy term values have to be obtained by diagonalizing an effective Hamiltonian matrix, rather than by a simple Dunham expansion. If inter-polyad interactions are ignored, the effective Hamiltonian matrix is block diagonalized for each polyad quantum number  $P$ . The diagonal matrix element, i.e., the zero-order unperturbed vibrational energy, can be expressed by a Dunham expansion as

$$\begin{aligned} \langle V_1, V_2^l, V_3 | \hat{H}^{\text{eff}} | V_1, V_2^l, V_3 \rangle \\ = G(V) = \sum_i \nu_i \left( V_i + \frac{d_i}{2} \right) \\ + \sum_{ij} \chi_{ij} \left( V_i + \frac{d_i}{2} \right) \left( V_j + \frac{d_j}{2} \right) + g_{22} l^2, \end{aligned} \quad (2)$$

where  $\hat{H}^{\text{eff}}$  refers to the effective Hamilton,  $\chi_{ij}$  and  $d_i$  are the anharmonic constant and the degeneracy of vibrational mode, respectively. Since in this experiment only vibrational levels of  $A^2\Sigma^+$  state with  $l=0$  (for even  $P$ ) or  $l=1$  (for odd  $P$ ) can be observed via excitation from the  $X^2\Pi(000)$  state, we may omit the small contribution of  $l=1$  to the vibrational energy in Eq. (2). The off-diagonal matrix elements for each block are<sup>26</sup>

$$\begin{aligned} \langle V_1, V_2^l, V_3 | \hat{H}^{\text{eff}} | V_1 + 1, (V_2 - 2)^l, V_3 \rangle \\ = \frac{1}{2\sqrt{2}} K_{122} \sqrt{(V_2 - l)^2 (V_1 + 1)}, \end{aligned} \quad (3)$$

$$\begin{aligned} \langle V_1, V_2^l, V_3 | \hat{H}^{\text{eff}} | V_1 + 2, V_2^l, V_3 - 1 \rangle \\ = \frac{1}{2\sqrt{2}} K_{113} \sqrt{V_3(V_1 + 1)(V_1 + 2)}, \end{aligned} \quad (4)$$

where  $K_{122}$  and  $K_{113}$  represent the constants of Fermi-resonance interactions between  $\nu_1$ ,  $\nu_2$  modes and  $\nu_1$ ,  $\nu_3$  modes, respectively. Here, we also ignore the higher order Fermi interactions, such as interactions between the  $(V_1, V_2, V_3)$  and  $(V_1 - 2, V_2 + 4, V_3)$  levels,  $(V_1, V_2, V_3)$  and  $(V_1, V_2 + 4, V_3 - 1)$  levels. Note that within the excitation energy range in this experiment, the  $\nu_3$  mode of the  $A^2\Sigma^+$  state can only be excited as high as  $V_3 = 3$ , the number of vibrational levels involving  $\nu_3$  mode are relatively less than those involving  $\nu_1$  and  $\nu_2$  modes, therefore, we also neglect the interaction between  $\nu_1$  and  $\nu_3$  modes, i.e., fix  $K_{113} = 0$ .

By diagonalizing the effective Hamilton matrix and fitting the identified transition peaks with a least-square procedure, the PHOFEX spectrum were assigned completely as the  $A^2\Sigma^+ [P, i] \leftarrow X^2\Pi_{3/2,1/2}(000)$  vibronic transitions, i.e., from the two spin-orbit sub-states of  $X^2\Pi(000)$  to the  $[P, i]$



TABLE II. Term values and the main components of  $[P, i]$  vibrational levels at the  $A^2\Sigma^+$  state of  $\text{N}_2\text{O}^+$ .

$[P, i]$	G(V) ( $\text{cm}^{-1}$ )			Main components (%)	References	
	Obs.	Cal.	Obs.-Cal.		Ref. 17	Ref. 18
4, 1	2432.5	2429.2	3.3	001(100)	2435	2450
4, 4	2687.6	2691.5	-3.9	200(97.1)	2680	2675
5, 4	3289.2	3288.1	1.1	210(92.8)		
6, 1	3654.0	3654.7	-0.7	021(98.6)		
6, 2	3670.6	3669.1	1.5	060(77.2), 140(21.8)		
6, 3	3772.9	3772.0	0.9	140(64.4), 060(22.0), 220(13.4)		
6, 5	3884.5	3881.9	2.6	220(81.8), 140(13.7)		
6, 6	4010.9	4012.9	-2.0	300(96.2)	4003	3997
7, 3	4367.0	4372.6	-5.6	150(47.0), 070(30.5), 230(21.7)		
7, 6	4600.6	4598.6	2.0	310(90.4), 230(9.0)		
8, 1&2	4869.0	4867.6 [8,1] 4871.9 [8,2]	1.4 -2.9	080(56.2), 160(38.1), 240(5.5) 041(92.6), 121(7.4)		
8, 3	4880.7	4881.9	-1.2	002(100)		4869
8, 6	5077.0	5070.3	6.7	240(46.7), 160(31.5), 320(16.5), 080(5.1)		
8, 8	5178.0	5181.4	-3.4	320(76.7), 240(17.2)		
8, 9	5322.4	5318.3	4.1	400(95.5)	5311	5316
9, 1	5466.6	5460.7	5.9	090(45.1), 170(44.3), 250(10.0)		
9, 6	5662.7	5663.4	-0.7	170(38.2), 250(25.5), 330(25.1), 090(10.0)		
9, 9	5890.1	5892.7	-2.6	410(88.7), 330(10.4)		
10, 1	6046.4	6049.5	-3.1	180(47.7), 0100(34.7), 260(16.0)		
10, 4	6163.2	6157.4	5.8	0100(46.9), 260(38.4), 340(11.5)		
10, 5	6183.0	6186.4	-3.4	141(68.0), 061(19.8), 221(12.1)		
11, 4	6739.6	6745.0	-5.4	0110(45.6), 270(33.4), 350(19.1)		
12, 2	7273.9	7271.7	2.2	081(60.0), 161(35.4)		
12, 8	7433.9	7432.6	1.3	122(91.1), 042(6.6)		

vibrational levels of the  $A^2\Sigma^+$  state, as indicated in Fig. 2. The assignment reconfirms that the initial states of the  $\text{N}_2\text{O}^+$  ions prepared through  $[3+1]$  REMPI at 360.55 nm are the vibrationless ground levels in the  $X^2\Pi_{3/2}$  and  $X^2\Pi_{1/2}$  sub-states, which is consistent to the previous photoelectron study by Scheper *et al.*<sup>25</sup>

The assignments for the  $A^2\Sigma^+ [P, i] \leftarrow X^2\Pi_{3/2, 1/2}(000)$  vibronic bands of  $\text{N}_2\text{O}^+$  resolved in Fig. 2 are summarized in Table I. For comparison, also listed in Table I are the observed peak positions in laser-induced photofragment study by Frey and co-workers,<sup>17</sup> which is the only laser excitation experiment in the present energy range. Totally 47 vibronic bands related to 24 vibrational levels of the  $A^2\Sigma^+$

state were identified in the present work, most of which were observed for the first time. The polyad number  $P$  for the observed vibrational levels of  $A^2\Sigma^+$  state ranges from 4 to 12. As can be seen in Fig. 2, the excitations of vibrational levels with odd  $P$ , i.e., zero-order levels with odd  $V_2$ , are observed. To the first-order approximation, the vibrational excitation of an odd quantum of  $V_2$  is forbidden in the linear  $A^2\Sigma^+ \leftarrow X^2\Pi(000)$  electronic transition. Such type of forbidden vibronic transitions with  $\Delta V_2 = \pm 1$  were also observed by Dehmer *et al.*<sup>20</sup> and Chen *et al.*<sup>18</sup> in their photoelectron studies and by Aarts and Callomon<sup>4</sup> in their fluorescence emission study, and was interpreted as vibronic interaction between the  $A^2\Sigma^+$  and  $X^2\Pi$  states.<sup>20</sup> This inter-

TABLE III. Spectral constants of the  $A^2\Sigma^+$  state determined from the global fit of the PHOFEX spectrum with consideration of Fermi-resonance interactions. All the values in the table are given in unit of  $\text{cm}^{-1}$ .

This work		References				
		Ref. 17	Ref. 3	Ref. 19	Ref. 18	Ref. 15
$\nu_1$	$1380.9 \pm 3.1$	1358	1345.52	$1360 \pm 15$	1346	
$\nu_2$	$627.3 \pm 1.8$		614.1		614	
$\nu_3$	$2433.0 \pm 7.4$		2451.7	$2470 \pm 15$	2452	
$\chi_{11}$	$-8.0 \pm 0.9$	-5.82				
$\chi_{22}$	$-0.4 \pm 0.2$					$-1.4^a$
$\chi_{33}$	$-11.8 \pm 4.0$					
$\chi_{12}$	$-13.1 \pm 1.1$					
$\chi_{23}$	$-3.6 \pm 0.9$					
$K_{122}$	$21.6 \pm 1.5$					
$T_0$	$28230 \pm 1$		28 229.94			
Spin-orbit splitting						
$X^2\Pi_{3/2, 1/2}$	$133.8 \pm 1.0$		132.36	130		

<sup>a</sup>Estimated value.

action, however, causes negligibly small shifts of the vibrational energy positions of the  $A^2\Sigma^+$  state compared to the Fermi-resonance interactions, as seen from Ref. 15. Therefore, it was not included in the  $A^2\Sigma^+$  Hamiltonian used to fit vibrational levels. As showed in Fig. 2, the forbidden bands are observed with considerable intensities despite their small Franck–Condon factors. This may be due to the high dissociation probabilities of the  $A^2\Sigma^+$  state. Detailed analysis about the photodissociation mechanism of  $A^2\Sigma^+$  state in this excitation energy range will be presented in another publication.

The term values of vibrational levels  $[P, i]$  at the  $A^2\Sigma^+$  state are summarized in Table II. The main fractions of the zero-order vibrational levels in each observed  $[P, i]$  level are also presented in the table, which equal to the coefficient squares in the eigenvectors derived from diagonalizing the effective Hamiltonian matrix. For comparison, several term values obtained in Refs. 17 and 18 are also listed in the table. Our results confirms the validity of previous works, not only the term values, but also the assignments without considering Fermi interaction, since it can be seen from Table II that these  $[P, i]$  levels consist of only one zero-order vibrational levels. However, for the newly observed  $[P, i]$  levels in this work, it is clearly seen that there exists a strong coupling between the  $\nu_1$  and  $\nu_2$  modes. Even though the Fermi interaction in the electronic ground  $X^2\Pi$  state have been extensively investigated in previous works,<sup>3–5,16,20</sup> there has been no report in the literature about the Fermi interaction in the excited  $A^2\Sigma^+$  state.

With the global fit to the observed vibronic bands, the spectral constants of the  $A^2\Sigma^+$  state were determined and the results are listed in Table III. The Fermi-interaction constant  $K_{122}$  was determined, for the first time, to be  $21.6 \pm 1.5 \text{ cm}^{-1}$ . The calculated vibrational term values of the  $A^2\Sigma^+$  state using these determined constants are listed in Table II. As seen in Table II, the differences between the calculated and observed values are less than  $6 \text{ cm}^{-1}$ , which should be acceptable for the vibrationally resolved spectrum. The spectral constants reported in literatures are also listed in Table III. Since in previous studies the anharmonic effect as well as the Fermi-resonance interaction were not considered due to the insufficient number of spectral data of the  $A^2\Sigma^+$  state, our determined vibrational frequencies are certainly different from those in literatures, especially the value of  $\nu_2$ . Furthermore, since many vibronic bands were identified in our PHOFEX spectrum, our spectral assignment should be more reliable, and the determined vibrational frequencies, the anharmonic constants and the Fermi-interaction constant should be in turn more precise.

#### IV. CONCLUSION

The spectroscopic studies of the  $A^2\Sigma^+$  state of  $\text{N}_2\text{O}^+$  ions were reported in present work. Pure parent ions of

$\text{N}_2\text{O}^+$  at the  $X^2\Pi_{3/2,1/2}(000)$  level, were prepared by  $[3+1]$  REMPI of neutral  $\text{N}_2\text{O}$  molecules at 360.55 nm, and were excited to various vibrational levels of the  $A^2\Sigma^+$  state by a tunable laser. The PHOFEX spectrum in the wavelength range of 278–328 nm was attributed completely to the  $A^2\Sigma^+ \leftarrow X^2\Pi$  electronic transition of  $\text{N}_2\text{O}^+$ , in which most vibronic bands were observed for the first time. By considering the Fermi resonance between the  $\nu_1$  and  $\nu_2$  modes, the spectrum was assigned, and the spectral constants of the  $A^2\Sigma^+$  state, such as vibrational frequencies, anharmonic constants and Fermi interaction constant, were obtained with relatively high reliability and precision.

#### ACKNOWLEDGMENTS

The present work was supported financially by the National Natural Science Foundation of China (#20273063) and the NKBRSF research program (#G1999075304).

- <sup>1</sup>J. D. Burley, K. M. Evin, and P. B. Armentrout, *J. Chem. Phys.* **86**, 1944 (1987).
- <sup>2</sup>N. Komiha, *J. Mol. Struct.* **306**, 313 (1994).
- <sup>3</sup>J. H. Callomon and F. Creutzberg, *Philos. Trans. R. Soc. London, Ser. A* **277**, 157 (1974).
- <sup>4</sup>J. F. M. Aarts and J. H. Callomon, *Chem. Phys. Lett.* **91**, 419 (1982).
- <sup>5</sup>C. E. Fellows and M. Vervloet, *Chem. Phys.* **264**, 203 (2001).
- <sup>6</sup>M. Tsuji and J. Maier, *Chem. Phys.* **126**, 435 (1988).
- <sup>7</sup>T. Imamura, T. Imajo, and I. Koyano, *J. Phys. Chem.* **99**, 15465 (1995).
- <sup>8</sup>I. Tokue, T. Kudo, and Y. Ito, *Chem. Phys. Lett.* **199**, 435 (1992).
- <sup>9</sup>T. Ibuki and N. Sugita, *J. Chem. Phys.* **80**, 4625 (1984).
- <sup>10</sup>I. Tokue, M. Kobayashi, and Y. Ito, *J. Chem. Phys.* **96**, 7458 (1992).
- <sup>11</sup>J. Lerme, S. Abed, M. Larzilliere, R. A. Holt, and M. Carre, *J. Chem. Phys.* **84**, 2167 (1986).
- <sup>12</sup>J. Lerme, S. Abed, R. A. Holt, M. Larzilliere, and M. Carre, *Chem. Phys. Lett.* **96**, 403 (1983).
- <sup>13</sup>M. Larzilliere, K. Gragued, J. Lerme, and J. B. Koffend, *Chem. Phys. Lett.* **134**, 467 (1987).
- <sup>14</sup>S. Abed, M. Broyer, M. Carre, M. L. Gaillard, and M. Larzilliere, *Chem. Phys.* **74**, 97 (1983).
- <sup>15</sup>M. Larzilliere and C. H. Jungen, *Mol. Phys.* **67**, 807 (1989).
- <sup>16</sup>M. Chafik el Idrissi, M. Larzilliere, and M. Carre, *J. Chem. Phys.* **100**, 204 (1994).
- <sup>17</sup>R. Frey, R. Kakoschke, and E. W. Schlag, *Chem. Phys. Lett.* **93**, 277 (1982).
- <sup>18</sup>W. Chen, J. Liu, and C. Y. Ng, *J. Phys. Chem. A* **107**, 8086 (2003).
- <sup>19</sup>R. Frey, B. Gotchev, W. B. Poatman, H. Pollak, and E. W. Schlag, *Chem. Phys. Lett.* **54**, 411 (1978).
- <sup>20</sup>P. M. Dehmer, J. L. Dehmer, and W. A. Chupka, *J. Chem. Phys.* **73**, 126 (1980).
- <sup>21</sup>H. Gritli, Z. B. Lakhdar, G. Chambaud, and P. Rosmus, *Chem. Phys.* **178**, 223 (1993).
- <sup>22</sup>G. Chambaud, H. Gritli, P. Rosmus, H. J. Werner, and P. J. Knowles, *Mol. Phys.* **98**, 1793 (2000).
- <sup>23</sup>L. Zhang, J. Chen, H. Xu, J. Dai, S. Liu, and X. Ma, *J. Chem. Phys.* **114**, 10768 (2001).
- <sup>24</sup>M. G. Szarka and S. C. Wallace, *J. Chem. Phys.* **95**, 2336 (1991).
- <sup>25</sup>C. R. Scheper, J. Kuijt, W. J. Buma, and C. A. deLange, *J. Chem. Phys.* **109**, 7844 (1998).
- <sup>26</sup>P. F. Bernath, M. Dulick, and R. W. Field, *J. Mol. Spectrosc.* **86**, 275 (1981).